Supporting Information

Gold Nanoparticles Bearing a Clinically Used None-antibiotic Drug for Combating Multi-drug Resistant Bacteria

*Yuexiao Jia,[1] Jiangjiang Zhang,[1] Yingcan Zhao,[1] Ruihua Dong,[1] Hui Wang[2] and Xingyu Jiang[1]**

[1] Guangdong Provincial Key Laboratory of Advanced Biomaterials, Shenzhen Key Laboratory of Smart Healthcare Engineering, Department of Biomedical Engineering, Southern University of Science and Technology, No. 1088, Xueyuan Rd., Xili, Nanshan District, Shenzhen, Guangdong, 518055, P. R. China.

[2] Department of Clinical Laboratory, Peking University People's Hospital, Beijing 100044, P. R. China.

* Correspondence: jiang@sustech.edu.cn

Experimental Procedures

Materials

$HAuCl_4 \cdot 3H_2O$ (99.99%), N-Acetyl-L-cysteine (NAC), cysteine, $NaBH_4$, glutaraldehyde, ethanol, osmic acid, uranyl acetate, lead citrate and all antibiotics were from Sigma. CCK-8, ATP, BCA protein, ROS assay kits were from Beyotime Institute of Biotechnology, China. Propidium iodide (PI) and $DiSC_3(5)$ were from Invitrogen Molecular Probes, Inc. Hematoxylin and eosin (H&E staining) and masson were from Beijing Bioss Biotechnology Co. LTD., China. PBS buffer, Luria-Bertani (LB) medium, Dulbecco's modified Eagle medium (DMEM) were from Solarbio life science, China.

Bacterial strains

Standard strains of *E. coli* (*Escherichia coli* (Migula) Castellani and Chalmers 11775™), *P. aeruginosa* (*Pseudomonas aeruginosa* (Schroeter) Migula27853) and *K. pneumonia* (*Klebsiella pneumoniae subsp. pneumoniae* (Schroeter) Trevisan13883) were from Genetimes Technology, Inc. Clinical MDR isolates, carbapenem-resistant *E. coli* (CR *E. coli*), and *K. pneumoniae* (CR *K. pneumoniae*), polymyxin-resistant *E. coli* (PR *E. coli*) and *K. pneumoniae* (PR *K. pneumonia*) were from local hospitals. We cultured bacteria in LB medium at 37 ℃ on a shaking bed at 220 rpm.

Synthesis of Gold nanoparticles

For the synthesis of Au_NAC nanoparticles, we mixed the aqueous solution of 5 mL $HAuCl_4 \cdot 3H_2O$ (5 mM) and 5 mL NAC (20 mM), stirred the solution for 10 min in the ice-water bath, and added the aqueous solution of 2.5 mL $NaBH_4$ (80 mM) dropwise. After an hour of gentle stirring, we purified NPs by dialysis (14 kDa MW cutoff) in deionized water for above 24 h and filtration by filters (0.22 mm). We optimized the synthesis parameters by changing the concentration of NAC (2.5, 5, 10, 20, 40, 80 mM) and $NaBH_4$ (20, 40, 80, 160, 320 mM). [1] For the synthesis of gold nanoparticles capped with NAC and stabilized with Tween 80 (Au_NAC_Tween), we mixed the aqueous solution of 5 mL $HAuCl_4 \cdot 3H_2O$ (5 mM), 5 mL NAC (20 mM), and 20 mg tween 80, stirred the solution for 10 min in the ice-water bath, and added the aqueous solution of 2.5 mL $NaBH_4$ (80 mM) dropwise. After an hour of gentle stirring, we purified NPs by dialysis (14 kDa MW cutoff) in deionized water for above 24 h and filtration by filters (0.22 mm). For the synthesis of Au NPs, we mixed the aqueous solution of 5 mL $HAuCl_4 \cdot 3H_2O$ (5 mM), 5 mL H_2O, and 20 mg Tween 80 (final concentration of 2 mg/mL), stirred the solution for 10 min in the ice-water bath, and added the aqueous solution of 2.5 mL $NaBH_4$ (40 mM) dropwise. After an hour of gentle stirring, we purified NPs by dialysis (14 kDa MW cutoff) in deionized water for above 24 h and filtration by filters (0.22 mm). For the synthesis of gold nanoparticles capped with cysteine (Au_C), we mixed the aqueous solution of 5 mL $HAuCl_4 \cdot 3H_2O$ (5 mM), 5 mL cysteine (20 mM), and 20 mg Tween 80, stirred the solution for 10 min in the ice-water bath, and added the aqueous solution of 2.5 mL $NaBH_4$ (40 mM) dropwise. After an hour of gentle stirring, we purified NPs by dialysis (14 kDa MW cutoff) in deionized water for above 24 h and filtration by filters (0.22 mm).

Characterization of Au_NAC

We determined the mass concentration of Au_NAC with inductively coupled plasma optical emission spectrometer (ICP-OES, Normal School of Beijing Elmer Optima 5300DV). We observed morphologies of NPs with transmission electron microscope (TEM, Tecnai G2 20 ST). We determined UV-vis absorption of the Au_NAC NPs solution with Daojin ultraviolet-visible spectrophotometer (UV-vis) and tested Zeta potential with Malvern Zetasizer Nano ZS. We analyzed elemental contents of the Au_NAC NPs through X-ray photoelectron spectroscopy (XPS, ESCALAB250Xi, Thermo Fisher).[1-4]

Minimum inhibitory concentration (MIC)

We determined the MIC using a microbroth dilution method according to CLSI guidelines.[5] We diluted the logarithmic-phase bacteria (OD_{600}≈0.1) with LB medium for a thousand folds. We added 100 μL of LB medium in every well of 96-well plate and then added 100 μL Au_NAC solution in the first well of each row. Au_NAC was diluted logarithmically in every row. We added 10 μL of bacterial suspension into each well with 100 μL of different concentrations of Au_NAC solutions. The plates were incubated in incubator at 37 ℃ for 24 h. MIC is the minimal concentration at which no bacterial turbid is observed in all three parallels after 24 h incubation at 37 ℃.[6] We evaluated the stability of Au_NAC. We stored Au_NAC solution in refrigerator at 4 ℃ for different times (1, 3, 5, 8, 15 months) and tested the MICs. We also stored Au_NAC powder after lyophilization at -20 ℃ for 1, 11, 25, 28 months and tested the MICs.

Morphological changes of *E. coli* treated with Au_NAC

We incubated *E. coli* with Au_NAC for 12 h and 24 h, fixed the bacteria for 3 h with 2.5% glutaraldehyde, and washed them with PBS. We dehydrated the samples by gradient ethanol solutions (30, 50, 70, 90, 95, 100%, v/v, in water) and dried them at room temperature. The group without Au_NAC was set as control. We used SEM to record the images. After 12 and 24 hours of treatment of *E. coli* with Au_NAC at 37 ℃, we fixed the bacteria with 2.5 % glutaraldehyde and 0.1 % osmic acid, dehydrated with graded ethanol, and further cut superthin slices and stained the slices with 2% uranyl acetate and 0.2 % lead citrate. The group without Au_NAC was set as control. We used TEM to record the images.[7]

Membrane proton motive force (PMF) of *E. coli*

E.coli was incubated with 4 μM $DiSC_3(5)$ for 1 h, ion-equilibrated with 100 mM KCl, then treated with Au_NAC for 1 h and the fluorescence was monitored with excitation at 622 nm and emission at 670 nm by Tecan infinite 200 microplate reader. The group without Au_NAC was a control.[8]

Intracellular ATP levels of *E. coli*

E.coli was treated with Au_NAC for 1 h. We collected the bacteria and detected intracellular ATP levels by an ATP assay kit. We lysed them with lysis buffer and centrifuged them at 12000 rpm for 5 min. The supernatant was divided into two parts. We added ATP-detecting solution to one part of the supernatant and immediately determine the luminescence with the Tecan infinite 200 microplate reader. The amount of protein in the other part of supernatant was detected by BCA protein assay kit. We corrected the ATP levels for different samples to nM/mg. The group without Au_NAC was set as control.[9]

Membrane permeability assay

We treated *E. coli* with Au_NAC for 12 and 24 h at 37 ^{o}C, and washed them with PBS. We stained the bacteria with PI (200 μM) for 30 min. The group without Au_NAC was set as control. We used confocal laser scanning microscope (CLSM, Olympus, FV1000-IX81) to record the fluorescent images. [10]

ROS productions

We tested the total ROS productions using Total Reactive Oxygen Species Test Kit. We stained the *E. coli* cells by stain solution for 30 min at 37 ^{o}C. Then the bacteria were washed and treated with Au_NAC for 1 h. The fluorescence was monitored with excitation at 488 nm and emission at 535 nm by Tecan infinite 200 microplate reader. The group without Au_NAC was set as control. [11]

Cytotocixity of Au_NAC

We tested the cytotocixity of Au_NAC using CCK-f8. HUVEC cells were cultured in DMEM for 24 h in a 96-well plate. We added different concentration of Au_NAC for 24 h. We discarded the supernatant and added 10 % (v/v) of the CCK-8 solution and incubated the sample at 37 °C for 2 h. We determined the absorbance at 450 nm using Tecan infinite 200 multimode microplate readers.

Hemolysis of Au_NAC

In hemolysis assay, human whole blood was centrifuged at 1200 r/min for 15 min. The supernatant was discarded, and physiological saline was used to wash RBCs three times, and to resuspend RBCs. Then we incubated RBCs (final concentration of 4 %) with different concentration of Au_NAC. H_2O was used as positive control and physiological saline was used as negative control. All samples were prepared in triplicates. After 3 h-incubation, we centrifuged them at 1200 r/min for 15 min, took pictures and analyzed the supernatant by UV-vis spectroscopy (Shimazu Spectrophotometer) at 540 nm.

***In vivo* toxicity of Au_NAC**

Balb/c mice (female 6-8 week) were bought from VITAL RIVER, Inc. We did a dose tolerance study of Au_NAC. Mice (six per group) were administered via a single intravenous dose of Au_NAC (0, 2.5, 5, 10, 20 and 40 mg/kg). Survival rates were monitored daily for 3 weeks. We investigated the distribution of Au_NAC in major organs. Mice were administered via an intravenous administration of Au_NAC (10 mg/kg) and sacrificed after 1, 4, 8, 24, and 36 h to obtain the major organs. The organs were weighed and dissolved using aqua regia for distribution studies. ICP-MS was used to measure the quantity of Au in organs. The experiments followed the relevant laws/institutional guidelines and were approved by the Institutional Animal Care and Use Committee, Southern University of Science and Technology (SUSTC-JY2019149).

***In vivo* efficacy**

We built a MDR bacterial wound infection model to test the *in vivo* efficacy of Au_NAC. We prepared full-thickness wounds with diameters of 2 cm on the dorsal side of Wistar rats (8 week). The wounds were infected by 200 μL CR *E. coli* (10^9 CFU/mL) for 30 min. We treated the infected wounds with gauze (control) and Au_NAC infiltrated gauze (Au_NAC). We monitored the wound healing progress in the control and Au_NAC groups and take photographs of the wounds at 0, 7, and 14 days. We collected the wound tissues and cultured the suspensions of grinded tissues on LB plates. We obtained the isometric continuum cut sections of each wound and stain them with H&E or Masson.[12] The experiments followed the relevant laws/institutional guidelines and were approved by the Institutional Animal Care and Use Committee, Institute of Process Engineering, Chinese Academy of Sciences (IPEAECA2018032).

Supporting Discussion

We compare the antibacterial activities of Au_NAC with Au NPs or Au_C (Table S1). Au NPs does not have antibacterial activity and its MICs are >3000 μg/mL. Gold nanoparticles capped with cysteine (Au_C), a derivative of NAC, does not show antibacterial activity. In contrast, when the gold nanoparticles are capped with NAC, the conjugates show excellent antibacterial activities against Gram-negative bacteria. To investigate the influence of Tween 80 on the antibacterial activities of gold nanoparticles, we synthesize NAC-capped gold nanoparticles stabilized with Tween 80 (Au_NAC_Tween) and test the antibacterial activities of Au_NAC_Tween. Au_NAC_Tween shows equivalent antibacterial activities against Gram-negative bacteria. Tween 80 does not influence the antibacterial activities of gold nanoparticles. We characterize Au NPs, Au_C, and Au_NAC_Tween nanoparticles. They possess similar particle sizes of 2.03±0.56 nm, 1.83±0.47 nm, and 1.85±0.50 nm. Their zeta potentials are –15.8±0.8 mV, –34.4±2.2 mV, and –33.2±4.5 mV. Au_NAC or Au_NAC_Tween have similar sizes and charges to Au_C, but they possess different antibacterial activities. So the presence of NAC is important for Au_NAC to exert antibacterial activities.

We evaluate the biocompatibility of Au_NAC before evaluating the *in vivo* efficacy. We test their effects on the viability of human umbilical vein endothelial cells (HUVECs). Au_NAC can keep 96.4 % cell viability at 64 μg/mL. Even at 128 μg/mL, 82.7 % HUVECs cells are alive after 24-h treatment (Figure S6). So the cytotoxicity of Au_NAC is acceptable. We carry out a hemolysis assay of Au_NAC and the results do not show obvious hemolysis for human erythrocytes even when the concentration of Au_NAC is 128 μg/mL (Figure S7). We also carry out a dose tolerance test to evaluate the *in vivo* toxicity of Au_NAC. Mice are challenged with a single intravenous dose of

Au_NAC and monitored for three weeks. We calculate the survival of mice and Au_NAC do not cause toxicity to mice even at 40 mg/kg (Figure S8). The low toxicity gives us confidence to develop Au_NAC as an antibacterial agent. We evaluate the distribution of Au_NAC in major organs (Figure S10). After an intravenous administration of Au_NAC (10 mg/kg), the Au levels in major organs are measured by ICP-MS. The results show that liver and spleen accumulate higher concentration of Au_NAC. So we think Au_NAC was likely metabolized via liver and spleen.

Table S1 Antibacterial activities of Au_NAC indicated by the MICs of Au+NAC, Au and NAC. Antibacterial activities of Au_NAC_Tween, Au NPs, and Au_C.

Organism	Au_NAC			Au_NAC_Tween	Au NPs	Au_C
	Au+NAC	Au	NAC			
E. coli	7.5	4	3.5	7	>3000	>3000
CR *E. coli*	15	8	7	14	>3000	>3000
PR *E. coli*	3.75	2	1.75	3.5	>3000	>3000
K. pneumoniae	7.5	4	3.5	7	>3000	>3000
CR *K. pneumoniae*	7.5	4	3.5	7	>3000	>3000
PR *K. pneumoniae*	15	8	7	14	>3000	>3000
P. aeruginosa	15	8	7	14	>3000	>3000

CR, carbapenem-resistant, PR, polymyxin-resistant, MIC, minimum inhibitory concentration (μg/mL). Au+NAC is the MICs of Au_NAC based on the total concentration of Au and NAC.

Table S2 Antibacterial activities of Au_NAC NPs with different ratio of Au and NAC or $NaBH_4$ indicated by MICs.

Organism	Au: $NaBH_4$ (1:X)						Au: NAC (1:Y)					
	2	4	8	12	16	24	0.5	1	2	4	8	16
E. coli	>128	9.5	**7.5**	14	25	>128	>128	64	44	**7.5**	18	>128
CR *E. coli*	>128	9.5	**15**	14	25	>128	>128	64	22	**15**	18	>128
PR *E. coli*	>128	19	**3.75**	14	25	>128	>128	16	22	**3.75**	36	>128
K. pneumoniae	>128	9.5	**7.5**	28	50	>128	>128	>128	22	**7.5**	18	>128
CR *K. pneumoniae*	>128	>128	**7.5**	56	100	>128	>128	16	11	**7.5**	18	>128
PR *K. pneumoniae*	>128	19	**15**	28	50	>128	>128	32	22	**15**	36	>128
P. aeruginosa	>128	>128	**15**	28	50	>128	>128	32	22	**15**	>128	>128

CR, carbapenem-resistant, PR, polymyxin-resistant, MIC, minimum inhibitory concentration (μg/mL). X is the molar ratio of $NaBH_4$ to Au. Y is the molar ratio of NAC to Au.

Table S3. Antimicrobial susceptibilities of Gram-negative bacteria indicated with MICs.

Organism	Antibiotics					
	Penicillin	Imipenem	Levofloxaci	Cefotaxime	Gentamicin	Polymyxin E
E. coli	4	2	<0.06	8	<0.06	0.5
CR *E. coli*	>128	32	32	>128	>128	4
PR *E. coli*	>128	>128	>128	0.125	<0.06	32
K. pneumoniae	4	8	0.13	2	0.13	2
CR *K. pneumoniae*	>128	>128	64	64	>128	2
PR *K. pneumoniae*	>128	>128	0.25	<0.06	>128	64
P. aeruginosa	8	8	2	4	8	1

CR, carbapenem-resistant, PR, polymyxin-resistant, MIC, minimum inhibitory concentration (μg/mL).

Table S4 Calculated ratios of Au and S, Au and NAC_{molar}, Au and NAC_{mass} in Au_NAC NPs.

Calculated Ratios	Au: $NaBH_4$ (1:X)				Au: NAC (1:Y)			
	4	8	12	16	1	2	4	8
Au : S	1: 1.09	1: 1.05	1: 1.62	1: 1.83	1: 0.86	1: 1.08	1: 1.05	1: 1.23
Au :	1: 1.09	1: 1.05	1: 1.62	1: 1.83	1: 0.86	1: 1.08	1: 1.05	1: 1.23
Au :	1: 0.90	1:0.87	1:1.34	1:1.52	1:0.71	1:0.89	1:0.87	1:1.02

Au : NAC_{malor}, molar ratio of Au and NAC, Au : NAC_{mass}, mass ratio of Au and NAC.

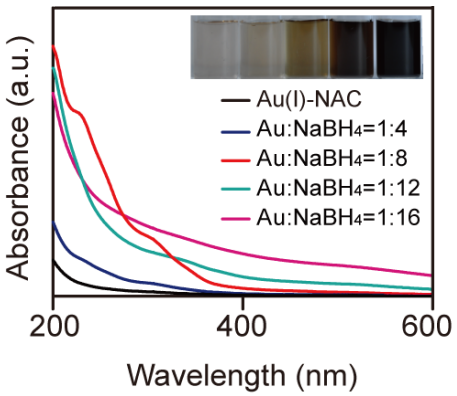

Figure S1 Photographs of Au(I)-NAC complex and Au_NAC NPs with different ratio of Au and $NaBH_4$.

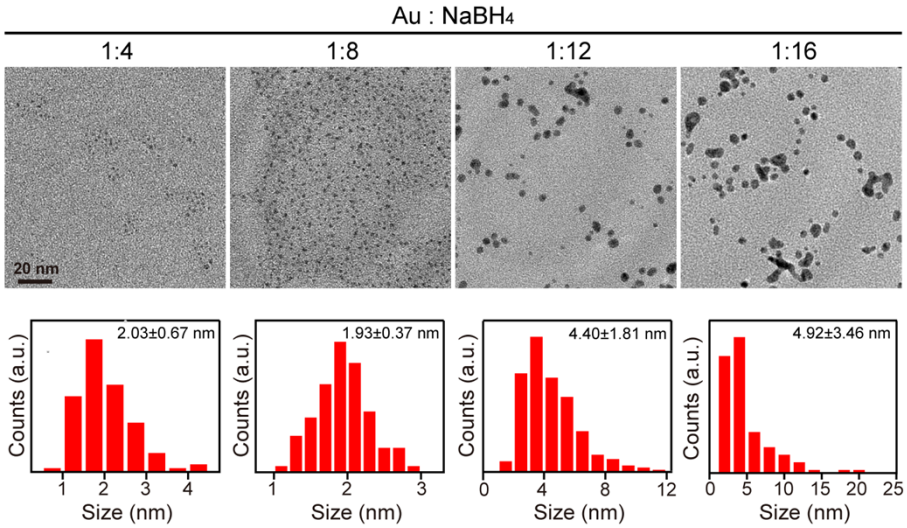

Figure S2 TEM image of Au_NAC NPs with different ratio of Au and $NaBH_4$.

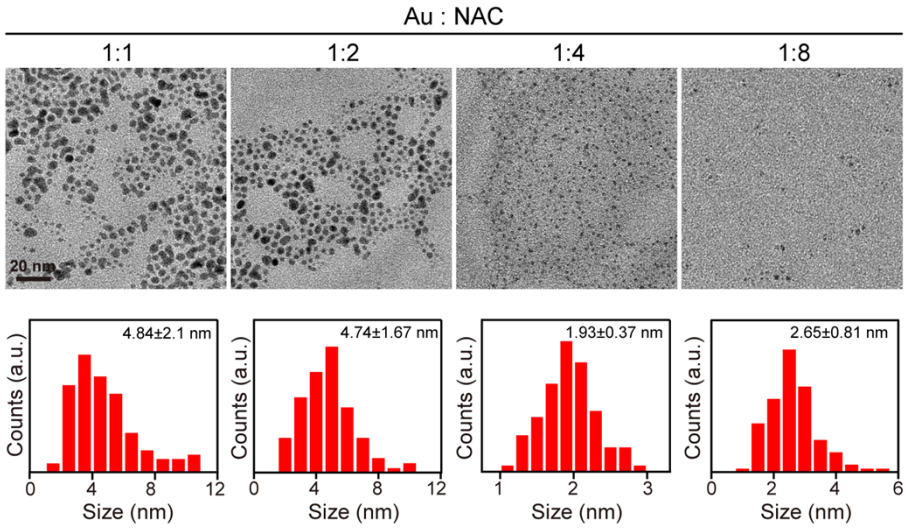

Figure S3 TEM image of Au_NAC NPs with different ratio of Au and NAC.

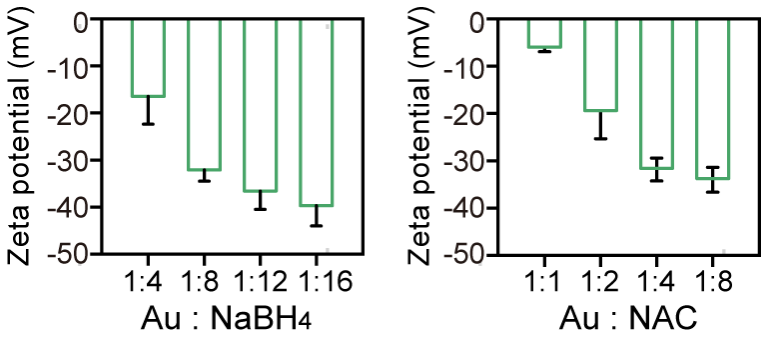

Figure S4 Zeta potential of Au_NAC NPs with different ratio of Au and $NaBH_4$ and different ratio of Au and NAC.

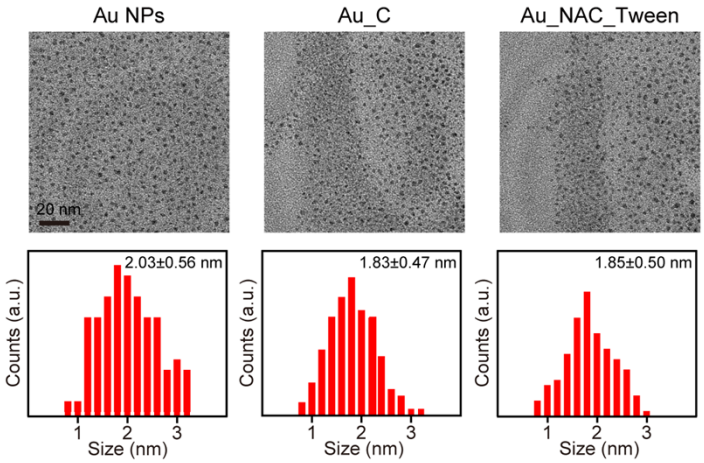

NPs	Zeta potential
Au NPs	–15.8±0.8 mV
Au_C	–34.4±2.2 mV
Au_NAC_Tween	–33.2±4.5 mV

Figure S5 TEM images, size distribution and zeta potential of Au NPs, Au _C, and Au_NAC_Tween.

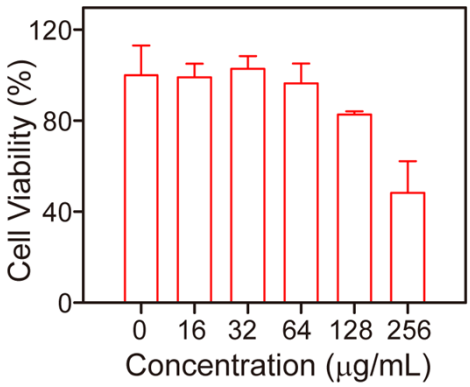

Figure S6 Cytotoxicity of Au_NAC on HUVECs.

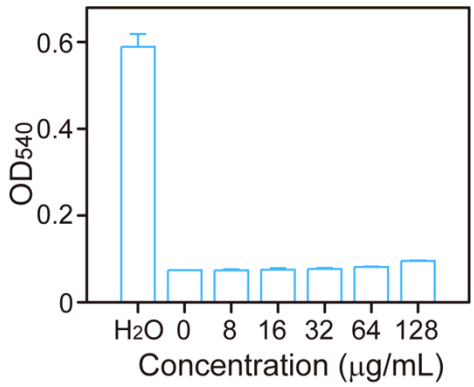

Figure S7 Hemolysis effects of Au_NAC.

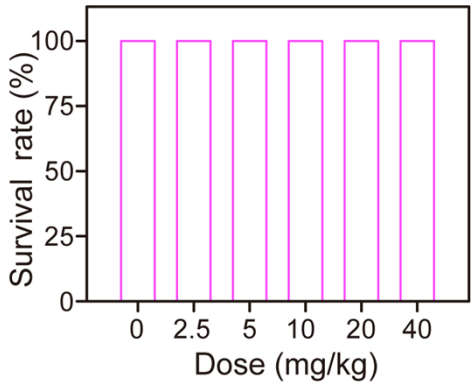

Figure S8 *In vivo* toxicity of Au_NAC.

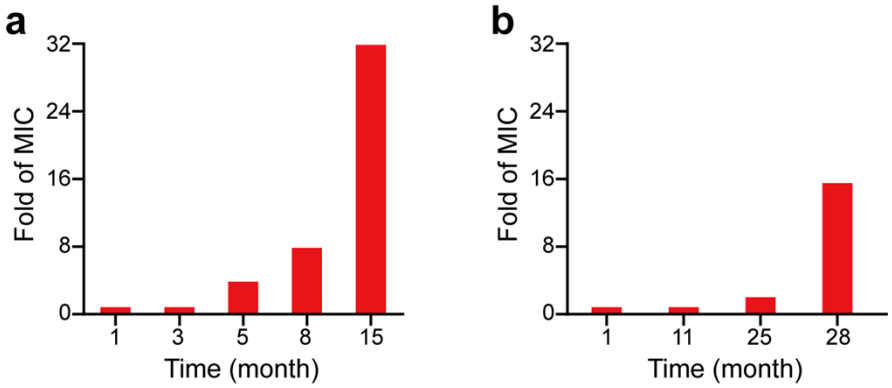

Figure S9 Stability of Au_NAC. Fold of MICs of Au_NAC after stored **a** at 4 ℃ in liquid condition and **b** at -20 ℃ in solid condition after lyophilization.

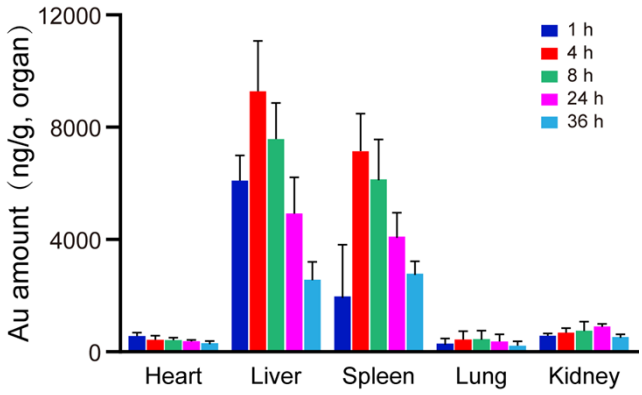

Figure S10 Quantitative analysis of Au amount per organ after intravenous administration.

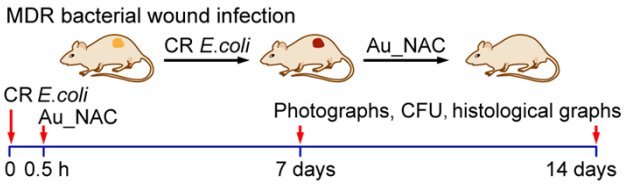

Figure S11 Scheme of the experimental protocol of MDR bacterial wound infections.

References

1. Zhao, Y. Y.; Tian, Y.; Cui, Y.; Liu, W. W.; Ma, W. S.; Jiang, X. Y., Small molecule-capped gold nanoparticles as potent antibacterial agents that target Gram-negative bacteria. *J. Am. Chem. Soc.* 2010, 132 (35), 12349-12356.
2. Zhao, Y. Y.; Chen, Z. L.; Chen, Y. F.; Xu, J.; Li, J. H.; Jiang, X. Y., Synergy of non-antibiotic drugs and pyrimidinethiol on gold nanoparticles against superbugs. *J. Am. Chem. Soc.* 2013, 135 (35), 12940-12943.
3. Zhang, J.; Mou, L.; Jiang, X., Hydrogels Incorporating Au@Polydopamine nanoparticles: robust performance for optical sensing. *Anal. Chem.* 2018, 90 (19), 11423-11430.
4. Corthey, G.; Giovanetti, L. J.; Ramallo-Lopez, J. M.; Zelaya, E.; Rubert, A. A.; Benitez, G. A.; Requejo, F. G.; Fonticelli, M. H.; Salvarezza, R. C., Synthesis and characterization of gold@gold(I) - thiomalate core@shell nanoparticles. *ACS Nano* 2010, 4 (6), 3413-3421.
5. CLSI Guidelines (2018) Performance Standards for Antimicrobial Susceptibility Testing. 28th Edition (M100S).
6. Greco, I.; Hummel, B. D.; Vasir, J.; Watts, J. L.; Koch, J.; Hansen, J. E.; Nielsen, H. M.;

Damborg, P.; Hansen, P. R., In vitro ADME properties of two novel antimicrobial peptoid-based compounds as potential agents against canine pyoderma. *Molecules* 2018, 23 (3).

7. Wang, L.; Li, S. X.; Yin, J. X.; Yang, J. C.; Li, Q. Z.; Zheng, W. F.; Liu, S. Q.; Jiang, X. Y., The density of surface coating can contribute to different antibacterial activities of gold nanoparticles. *Nano Lett.* 2020, 20 (7), 5036-5042.
8. Farha, M. A.; Verschoor, C. P.; Bowdish, D.; Brown, E. D., Collapsing the proton motive force to identify synergistic combinations against *Staphylococcus aureus*. *Chem. Biol.* 2013, 20 (9), 1168-78.
9. Zhao, X. H.; Jia, Y. X.; Dong, R. H.; Deng, J. Q.; Tang, H.; Hu, F. P.; Liu, S. Q.; Jiang, X. Y., Bimetallic nanoparticles against multi-drug resistant bacteria. *Chem. Commun.* 2020, 56 (74), 10918-10921.
10. Zhao, X.; Jia, Y.; Li, J.; Dong, R.; Zhang, J.; Ma, C.; Wang, H.; Rui, Y.; Jiang, X., Indole derivative-capped gold nanoparticles as an effective bactericide *in vivo*. *ACS Appl. Mater. Interfaces.* 2018, 10 (35), 29398-29406.
11. Xie, Y.; Liu, Y.; Yang, J.; Liu, Y.; Hu, F.; Zhu, K.; Jiang, X., Gold nanoclusters for targeting methicillin-resistant *Staphylococcus aureus in vivo*. *Angew. Chem. Int. Ed. Engl.* 2018, 57 (15), 3958-3962.
12. Yang, X. L.; Yang, J. C.; Wang, L.; Ran, B.; Jia, Y. X.; Zhang, L. M.; Yang, G.; Shao, H. W.; Jiang, X. Y., Pharmaceutical intermediate-modified gold nanoparticles: against multidrug-resistant bacteria and wound-healing application via an electrospun scaffold. *ACS Nano* 2017, 11 (6), 5737-5745.